

## Conserved Active Site Residues Limit Inhibition of a Copper-Containing Nitrite Reductase by Small Molecules<sup>†,‡</sup>

Elitza I. Tocheva, Lindsay D. Eltis, and Michael E. P. Murphy\*

Department of Microbiology and Immunology, Life Sciences Institute, University of British Columbia, 2350 Health Sciences Mall, Vancouver BC, V6T 1Z3, Canada

Received October 12, 2007; Revised Manuscript Received February 20, 2008

**ABSTRACT:** The interaction of copper-containing dissimilatory nitrite reductase from *Alcaligenes faecalis* S-6 (AfNiR) with each of five small molecules was studied using crystallography and steady-state kinetics. Structural studies revealed that each small molecule interacted with the oxidized catalytic type 2 copper of AfNiR. Three small molecules (formate, acetate and nitrate) mimic the substrate by having at least two oxygen atoms for bidentate coordination to the type 2 copper atom. These three anions bound to the copper ion in the same asymmetric, bidentate manner as nitrite. Consistent with their weak inhibition of the enzyme ( $K_i > 50$  mM), the Cu–O distances in these AfNiR–inhibitor complexes were  $\sim 0.15$  Å longer than that observed in the AfNiR–nitrite complex. The binding mode of each inhibitor is determined in part by steric interactions with the side chain of active site residue Ile257. Moreover, the side chain of Asp98, a conserved residue that hydrogen bonds to type 2 copper-bound nitrite and nitric oxide, was either disordered or pointed away from the inhibitors. Acetate and formate inhibited AfNiR in a mixed fashion, consistent with the occurrence of second acetate binding site in the AfNiR–acetate complex that occludes access to the type 2 copper. A fourth small molecule, nitrous oxide, bound to the oxidized metal in a side-on fashion reminiscent of nitric oxide to the reduced copper. Nevertheless, nitrous oxide bound at a farther distance from the metal. The fifth small molecule, azide, inhibited the reduction of nitrite by AfNiR most strongly ( $K_{ic} = 2.0 \pm 0.1$  mM). This ligand bound to the type 2 copper center end-on with a Cu–N<sub>c</sub> distance of  $\sim 2$  Å, and was the only inhibitor to form a hydrogen bond with Asp98. Overall, the data substantiate the roles of Asp98 and Ile257 in discriminating substrate from other small anions.

Copper-containing nitrite reductase (NiR<sup>1</sup>) catalyzes the one electron reduction of nitrite to nitric oxide. This reaction is the committing step in the denitrification pathway employed by a variety of bacteria to generate energy during anoxic conditions (1). NiR is a homotrimer with two, spectroscopically distinguishable copper ions per subunit (2, 3). The type 1 copper site is located near the surface of the

protein, and it receives electrons from a physiological electron donor, such as pseudoazurin (4). The electrons are then passed onto the type 2 copper site, which is the catalytic center. The latter is located at the bottom of a 16 Å deep cavity at the interface between two adjacent subunits. The two copper centers are 12 Å apart but are connected via a cysteinyl ligand of the type 1 center and a histidyl ligand of the type 2 center. This Cys–His bridge is thought to ensure efficient electron transfer between the copper centers.

Kinetic, crystallographic and spectroscopic studies have provided considerable insight into the catalytic mechanism of NiR, which involves changes in the oxidation state of both copper centers and changes in ligand coordination of the type 2 center (5). In the resting state of the enzyme, both copper ions are oxidized and the type 2 center is coordinated by three histidine residues and a water molecule (2, 3, 6). Recent steady-state kinetic studies indicate that the enzyme employs a random-sequential mechanism dependent on nitrite concentration and pH (7). In the first step of the proposed mechanism nitrite binds to either the reduced or oxidized type 2 copper. Crystallographic studies of the NiR–nitrite complex revealed that nitrite is bound asymmetrically to the oxidized type 2 copper, with Cu–O distances of 2.0 Å and 2.3 Å, suggesting that the more distant oxygen atom, O<sub>nc</sub>, is likely noncoordinating (6, 8, 9). Electron transfer from the type 1 copper or binding of nitrite to the reduced type 2 copper likely triggers rearrangement at the active site to

<sup>†</sup> This work was supported by NSERC Discovery Grants to L.D.E. and M.E.P.M. and a UBC University Graduate Fellowship (E.I.T.). Portions of this research were carried out at the Stanford Synchrotron Radiation Laboratory, a national user facility operated by Stanford University on behalf of the U.S. Department of Energy, Office of Basic Energy Sciences. The SSRL Structural Molecular Biology Program is supported by the Department of Energy, Office of Biological and Environmental Research, and by the National Institutes of Health, National Center for Research Resources, Biomedical Technology Program.

<sup>‡</sup> The atomic coordinates of AfNiR complexes with each of azide, formate, nitrate, acetate and nitrous oxide have been deposited in the PDB as entries 2E86, 2PP8, 2PP9, 2PP7 and 2PPA, respectively.

\* To whom correspondence should be addressed. Tel: 604-822-8022. Fax: 604-822-6041. E-mail: Michael.Murphy@ubc.ca.

<sup>1</sup> Abbreviations: NiR, copper-containing nitrite reductase; AfNiR, nitrite reductase from the bacterium *Alcaligenes faecalis* S-6; AcNiR, nitrite reductase from *Achromobacter cycloclastes*; AxNiR, nitrite reductase from *Alcaligenes xylooxidans*; Cu–O<sub>c</sub>, an oxygen atom coordinating to the type 2 copper; Cu–O<sub>nc</sub>, an oxygen atom interacting with but considered noncoordinating to the copper (Cu–O distance  $> 2.1$  Å); Cu–N<sub>c</sub>, nitrogen atom coordinating to type 2 copper; EPR, electron paramagnetic resonance; D98N, Asp98Asn variant of AfNiR; H145A, His145Ala variant of AfNiR; SSRL, Stanford Synchrotron Radiation Laboratory.

produce nitric oxide and water. A copper–nitrosyl intermediate of undetermined structure has been proposed, although a recent study showed that nitric oxide may coordinate to copper in a side-on fashion (9). Such a binding mode would obviate the need for flipping of the nitric oxide molecule at the active site from O- to N-coordination. Finally, the mechanism of NO release to return the enzyme to its resting state is also unknown.

Structural and mutagenesis studies indicate that three highly conserved active site residues determine the binding mode of nitrite and nitric oxide at the type 2 copper center: Asp98, Ile257 and His255 (10, 11). Asp98 appears to stabilize the binding of nitrite at the active site via a hydrogen bond between the O $\delta$ 1 atom of the former and the O $\epsilon$  atom of the latter (8). Substitution of Asp98 with Asn disrupts this hydrogen bond, weakening nitrite binding (12–14) and decreasing the specific activity of the enzyme (15). Moreover, Asp98 stabilizes the side-on binding of nitric oxide to the reduced type 2 copper site of NiR (9, 16). Ile257, positioned within 3 Å from the bound substrate and product, is one of several bulky hydrophobic residues that help shape the active site. Substitutions of Ile257 decreased the specific activity of NiR and weakened the binding of nitrite (11, 17).

Herein, we investigated the interaction of a five small molecules with AfNiR to gain insight into the mechanism of inhibition of such enzymes. Three small molecules were chosen based on the presence of two oxygen atoms for potential bidentate coordination to the type 2 copper: acetate, formate and nitrate. The two others, azide and nitrous oxide, were chosen based on the presence of nitrogen atoms and the linearity of the molecules. Interactions of the studied anions with AfNiR were examined by X-ray crystallography and steady-state kinetics. Analyses of the data provide insight into the molecular basis of how NiR discriminates against small charged molecules that mimic substrates or may act as inhibitors. The role of Asp98 and Ile257 in excluding metabolites that are potential inhibitors is described.

## EXPERIMENTAL PROCEDURES

**Protein Expression and Purification.** Recombinant AfNiR was expressed in *Escherichia coli* BL21 (DE3) cells (Novagen) as previously described (15, 18) with the following modifications. Briefly, cells were grown using 2 $\times$  YT (Difco) supplemented with 25  $\mu$ g/mL kanamycin at 30 °C. When the culture reached an OD<sub>600</sub> of 1.2, 0.5 mM IPTG was added and the culture was incubated at 25 °C overnight. Cells were harvested, supplemented with 50  $\mu$ M CuSO<sub>4</sub> and lysed at 4 °C using an Avestin EmulsiFlex-C5 homogenizer. The soluble fraction was applied to a Ni-Sepharose 6 Fast flow resin column (GE Healthcare), and the protein was eluted using 180 mM imidazole. The histidine tag was removed by digestion with bovine alpha thrombin (Haematologics Technologies) in 20 mM Tris-HCl, pH 7.0. The AfNiR protein was then applied to a Resource Q anion exchange column (GE Healthcare) and eluted with increasing salt concentration. The yield of purified AfNiR was 150 mg per L of bacterial culture. The A<sub>277</sub>/A<sub>593</sub> ratio was 2.0, similar to the value reported for the pure native protein (19). Protein concentrations were calculated using Bradford assay. The copper content was 1.7 Cu atoms per monomer as determined using bicinchoninic acid (20, 21).

**Enzymatic Assays.** The AfNiR-catalyzed reduction of nitrite was measured by following the oxidation of pseudoazurin at 593 nm using a Cary Varian 5000 spectrophotometer equipped with a Pelletier cooling device operated at 25 °C. Steady-state kinetic assays were performed in a final volume of 150  $\mu$ L containing 0.23 nM AfNiR, 40–800  $\mu$ M nitrite, saturating amounts of reduced pseudoazurin (>315  $\mu$ M), and 50 mM MES, pH 6.5. For reactions performed at pH 4, the assay contained 12 nM AfNiR, 2.5–100  $\mu$ M nitrite, and 10 mM benzoate. Dilutions of AfNiR were supplemented with 0.1 mg/mL BSA to stabilize the trimeric form of the enzyme. Reduced pseudoazurin was prepared in a dry box maintained at <2 ppm of O<sub>2</sub>. Pseudoazurin was reduced using ascorbate. Excess ascorbate was removed by passing the sample over a small column of Sephadex G-25 (GE Healthcare) equilibrated with the reaction buffer. The concentration of pseudoazurin was determined by completely oxidizing the protein with K<sub>3</sub>[Fe(CN)<sub>6</sub>] and using an extinction coefficient of 2900 M<sup>-1</sup> cm<sup>-1</sup> at 593 nm (21). Steady-state inhibition parameters were evaluated using the conditions described above and concentrations of 0.5–10 mM azide, and 10–500 mM of each of acetate, nitrate and formate. Steady-state kinetic parameters were calculated using initial rates determined over 5 s. Initial rates were corrected for the nonenzymatic rate of oxidation of pseudoazurin by nitrite, which never exceeded 10% of the enzymatic rate. Steady-state rate equations were fitted to data using the least-squares and dynamic-weighting options of the program LEONORA (22).

**Crystallization and Structure Solution.** Native AfNiR crystals were grown at room temperature by the hanging-drop vapor diffusion method in a reservoir containing 6–10% PEG 4000, 100 mM sodium acetate, pH 4. Each drop was made from an equal volume of reservoir and a 25 mg/mL protein stock solution containing 20 mM Tris-HCl, pH 7.0. The AfNiR crystals were soaked aerobically for 30 min in reservoir solution supplemented to 20 mM of azide, formate or nitrate. The concentration of acetate used in the acetate-bound AfNiR structure was 100 mM (part of the reservoir solution), and the manipulation of these crystals was performed anaerobically. Crystals of the nitrous oxide bound AfNiR were also manipulated anaerobically as described previously (9). Both reduced and oxidized AfNiR crystals were soaked in nitrous oxide saturated solutions (the nitrous oxide solubility in aqueous solutions is 25 mM at 1 atm, 25 °C (23)); however, after refinement only the oxidized crystals showed density for a nitrous oxide molecule bound to the type 2 copper of AfNiR. The data set of the oxidized NiR exposed to N<sub>2</sub>O was processed with a high overall *R*<sub>merge</sub> factor (Table 1) indicative of distortion of the crystal lattice when exposed to nitrous oxide or radiation damage during data collection. Prior to immersing in liquid nitrogen, all crystals were transferred to reservoir solution supplemented to 30% (v/v) glycerol and diffraction data were collected at 100 K. Data sets were collected on beamline 7-1 (for azide- and formate-bound AfNiR complexes) and at beamline 11-3 (for the nitrous oxide bound AfNiR complex) at the Stanford Synchrotron Radiation Laboratory (Menlo Park, CA). The acetate- and nitrate-bound AfNiR data sets were collected at a home source. All data sets were collected to 1.8 Å or better resolution and were indexed, scaled and merged with DENZO and SCALEPACK (24). Data collection statistics are summarized in Table 1.

Table 1: Data Collection and Refinement Statistics for the AfNiR–Inhibitor Complexes<sup>a</sup>

	NiR–azide	NiR–formate	NiR–nitrate	NiR–acetate	NiR–N <sub>2</sub> O
	Data Collection				
resolution (Å)	30–1.50 (1.54–1.50)	30–1.50 (1.55–1.50)	30–1.8 (1.85–1.8)	30–1.65 (1.71–1.65)	30–1.7 (1.76–1.7)
space group	<i>P</i> 2 <sub>1</sub> 2 <sub>1</sub> 2 <sub>1</sub>				
unit cell dimensions (Å)	<i>a</i> = 61.8 <i>b</i> = 102.6 <i>c</i> = 146.0	<i>a</i> = 61.3 <i>b</i> = 102.5 <i>c</i> = 146.2	<i>a</i> = 61.0 <i>b</i> = 102.1 <i>c</i> = 145.8	<i>a</i> = 61.0 <i>b</i> = 102.2 <i>c</i> = 146.1	<i>a</i> = 60.7 <i>b</i> = 101.6 <i>c</i> = 146.1
unique reflections	137746	126965	76833	100105	91791
completeness (%)	97.5 (99.5)	90.4 (80.8)	95.4 (92.4)	96.2 (89.4)	97.8 (97.2)
average <i>I</i> / <i>σ</i> <i>I</i>	17.5 (5.9)	24.8 (2.0)	21 (4.0)	22.7 (5.1)	15.2 (4.7)
redundancy	3.9	3.6	5.0	6.2	4.8
<i>R</i> <sub>merge</sub> <sup>b</sup> (%)	5.2 (20.2)	3.7 (45.1)	8.8 (42.8)	8.6 (36.1)	12.7 (37.8)
	Refinement				
<i>R</i> <sub>work</sub> / <i>R</i> <sub>free</sub> (%)	16.0/18.0 (19.0/23.0)	16.4/20.1 (28.7/38.5)	16.9/19.5 (27.7/33.0)	15.3/17.9 (20.2/23.3)	19.1/22.4 (25.7/31.2)
<i>B</i> -value (Å <sup>2</sup> )					
overall	15	19	21	20	24
Cu atoms	10	15	20	15	19
coordinate error <sup>c</sup> (Å)	0.04	0.05	0.08	0.06	0.08
rms deviation from ideality					
bond lengths (Å)	0.006	0.010	0.012	0.010	0.009
bond angles (deg)	1.096	1.288	1.330	1.342	1.308
PDB code	2E86	2PP8	2PP9	2PP7	2PPA

<sup>a</sup> Numbers in parentheses correspond to those in the highest resolution shell. Data was collected at 100 K. <sup>b</sup>  $R_{\text{merge}} = \sum(|I - \langle I \rangle|) / \sum(I)$  where, for each unique reflection, *I* is the intensity for each observation, and  $\langle I \rangle$  is the mean intensity. <sup>c</sup> Coordinate error derived from maximum likelihood refinement.

**Structure Refinement.** The inhibitor-bound crystals of AfNiR grew in space group *P*2<sub>1</sub>2<sub>1</sub>2<sub>1</sub> with a trimer in the asymmetric unit and were isomorphous with previous AfNiR crystal structures (3, 25). The 1.3 Å resolution NO-soaked native AfNiR structure (PDB code 1SNR) was used as the starting model following removal of all solvent atoms, the side chain of Asp98 and the NO molecule. In the final structures, each chain begins at Ala4 and ends at Glu339. Standard maximum likelihood positional and *B*-refinement was carried out using the program REFMAC (26). Solvent was added with the ARP/wARP program (27) from the CCP4 package (28), resulting in an *R*<sub>work</sub> below 17% and an *R*<sub>free</sub> of less than 22% for each of the five structures. During refinement, the interactions between copper and the inhibitor and between copper and the polypeptide chain were not restrained. Manual intervention was accomplished using the visualization program O (29). Over 95% of the residues in each structure occupy the most favorable position with the remaining residues in the allowed regions in a Ramachandran plot as described by PROCHECK (30). Final refinement statistics are presented in Table 1.

## RESULTS

Structural analyses revealed that AfNiR bound each of the five small molecules tested. In each of the binary complexes, the major differences were localized around the type 2 copper sites, as described below. The overall protein folds of the complexes were essentially identical when compared to the native AfNiR crystal structure (PDB entry 1AS7) as revealed by a rms deviation between the C $\alpha$  atoms of less than 0.2 Å.

**Active Site Structure and Inhibitor Binding.** The *F*<sub>o</sub> – *F*<sub>c</sub> difference map of the azide-exposed oxidized AfNiR crystal structure to 1.5 Å resolution revealed an elongated difference electron density in close proximity to the active site metal of each monomer, which was assigned to an azide anion (Figure 1A). Azide was modeled coordinating to the type 2 copper by one of its terminal nitrogen atoms in an end-on

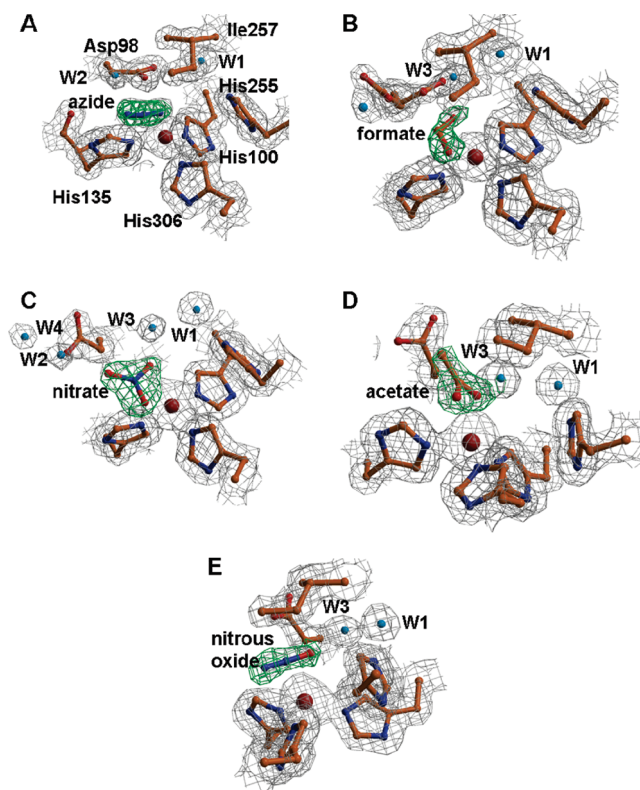


FIGURE 1: Inhibitors bound to type 2 Cu of AfNiR. Stick diagram of the coordination geometries at the type 2 copper center showing (A) azide binding, (B) formate binding, (C) nitrate binding, (D) acetate binding, (E) nitrous oxide binding. The  $2F_o - F_c$  electron density map is colored in gray and contoured at  $1\sigma$ . The omit difference electron density map is colored in green and contoured at  $4\sigma$ . The residues surrounding the copper atom are labeled in panel A. Nitrogen atoms are colored in blue, oxygen atoms are colored in red, carbon atoms are colored in yellow and water molecules are colored in cyan. Ile257 has been omitted from panel C for clarity. Molscript (43) and Raster3D (44) were used to prepare the figure.

Table 2: Range of Distances between Exogenous Ligand and Type 2 Copper of *AfNiR*–Inhibitor Complexes

parameter	<i>AfNiR</i> –nitrite <sup>a</sup>	<i>AfNiR</i> –nitric oxide <sup>a</sup>	formate	acetate	nitrate	azide	nitrous oxide
O <sub>c</sub> –Cu	2.04–2.08	n/a	2.19	2.12–2.16	2.10–2.22	n/a	2.06–2.17 <sup>d</sup>
N–Cu	2.31–2.36	1.97–2.01	2.52 <sup>b</sup>	2.49–2.53 <sup>b</sup>	2.48–2.51	1.97–2.08	2.10–2.20
O <sub>nc</sub> –Cu	2.29–2.38	1.95–2.12	2.39	2.38–2.42	2.21–2.29	n/a	2.47–2.67 <sup>e</sup>
O <sub>c</sub> –Oδ1 Asp98	2.53–2.66	2.50–2.65	2.41	n/a	n/a	2.94–3.15 <sup>c</sup>	n/a

<sup>a</sup> From ref 9. <sup>b</sup> Ligand distance for carbon atom. <sup>c</sup> Distance between Asp98 and N<sub>c</sub> atom of azide. <sup>d</sup> Range for subunits A and B only. <sup>e</sup> Ligand distance for the second nitrogen in nitrous oxide.

mode with a Cu–N<sub>c</sub> distance of 1.97–2.08 Å (range over 3 monomers). The molecule also interacts with residues surrounding the active site. The distance between the Oδ1 atom of Asp98 and the coordinating N<sub>c</sub> atom of azide is 2.94–3.15 Å. The Cu–N–N angle is 119°, apparently due to a steric clash with Ile257 (~3.3 Å). The most distal nitrogen atom of azide forms a hydrogen bond (~3.0 Å) with a water molecule (W2, Figure 1A), which in turn forms a hydrogen bond to the Oδ1 atom of Asp98 (~2.5 Å). Azide was modeled at full occupancy at each active site and refined with a final average *B*-factor of 27 Å<sup>2</sup>.

The binding of formate to oxidized *AfNiR* crystals was slightly different in each of the subunits. In subunit A, a difference map revealed electron density that can accommodate at most three atoms in a nonlinear fashion (Figure 1B). Formate was modeled at full occupancy and refined coordinating to the type 2 copper via one of its oxygen atoms (Cu–O<sub>c</sub> distance of 2.19 Å). In the final model, the second oxygen and carbon atoms are situated 2.39 and 2.52 Å from the copper ion, respectively. The side chain of Asp98 is disordered and was modeled in two distinct conformations at 50% occupancy each. In the inward position, the carboxylate group is pointing toward the copper and may form a hydrogen bond with the O<sub>c</sub> atom of formate. A rotation of approximately 80° about the χ<sub>2</sub> torsional angle gives an outward conformation resulting in the Oδ2 atom being displaced about 3.8 Å. The displacement of the side chain of Asp98 results in a pocket which is occupied by a solvent molecule (W3), refined at 50% occupancy. The two conformations of Asp98 are also observed in subunits B and C. However, in these subunits, the bound formate was more disordered, with two predominant binding modes. In addition to the mode observed in subunit A, subunits B and C show a second weaker interaction of formate to the metal with a Cu–O distance of 2.4 Å (see Supporting Information Figure S1, Table 2). The second formate conformation may be stabilized by a hydrogen bond with a nearby water molecule (~2.7 Å), which is also hydrogen bonded to the Oδ1 atom of the Asp98 (2.6 Å). Each of the binding modes was refined at 50% occupancy and resulted in an average *B*-factor of 28 Å<sup>2</sup>.

In crystals of *AfNiR* exposed to nitrate, a molecule of this inhibitor was modeled in the difference electron density observed at the type 2 copper site (Figure 1C). In the model, two of nitrate's three oxygen atoms are situated 2.19 and 2.23 Å away from the metal, respectively, consistent with bidentate binding. As described below, acetate can also bind to the type 2 site. However, three lines of evidence indicate that the bound molecule in this structure is nitrate: (1) when acetate was refined in the observed electron density, the *B*-values were on average 5 Å<sup>2</sup> larger; (2) nitrate fitted better to the calculated difference map due to the presence of three electronically equivalent oxygen atoms; and (3) the water

network and anion-binding modes near the active site differ from those observed in the NiR–acetate structure described below. In the NiR–nitrate complex, Ile257 occludes the active site, constraining the nitrate to bind at a 25° angle with respect to the plane defined by the oxygen atoms and the copper ion. The side chain of Asp98 points away from the copper, presumably due to the bulkiness of the inhibitor molecule. A hydrogen bond network comprising water molecules surrounds the bound anion. One of these water molecules, W3, occupies the free space created by the displacement of the Asp98 carboxylate and is situated 2.7 Å from one of the oxygen atoms of nitrate (Figure 1C). As observed in the NiR–formate complex, W3 stabilizes the bridging water (W1) by a hydrogen bond (2.7 Å) such that no changes were observed in the orientation of His255. The water network interacting with the bound nitrate extends to two other water molecules: W2 and W4 are situated 3.3 Å and 2.7 Å away from nitrate and Asp98, respectively.

Anaerobically manipulated crystals of oxidized *AfNiR* prepared at pH 4 had acetate bound at the type 2 copper site as indicated by the difference electron density map (Figure 1D). This is in contrast to the water molecule that occupies the fourth coordination position of the type 2 copper in the resting state of the crystallized enzyme (3), despite the fact that acetate was a component of the crystallization buffer in both experiments. To investigate the origin of this difference, two additional data sets of *AfNiR* were prepared at pH 4 and pH 6.5, respectively, and data were collected aerobically (data not shown). These data sets revealed that the presence of acetate coordinating to the type 2 copper in the crystallized enzyme is due to the acidic pH and not the absence of oxygen. A water molecule occupies the fourth coordination position of the type 2 copper at pH 6.5. In crystals prepared at pH 4, an acetate molecule was refined at full occupancy coordinating to the copper via its two oxygen atoms that are situated 2.12–2.16 Å and 2.38–2.42 Å (range over 3 monomers) away from the metal. Binding of acetate at the active site requires that the side chain of Asp98 swings away from the copper. A hydrogen bond is formed between the acetate and a nearby water molecule, W3 (~2.8 Å). No disorder in the binding mode of acetate at the active site is observed, and the three acetate molecules were modeled in at full occupancy and refined to an average *B*-factor of 26 Å<sup>2</sup>.

Crystals of the reduced and oxidized *AfNiR* exposed to nitrous oxide were also examined by X-ray diffraction. The reduced crystals exposed to nitrous oxide revealed no difference peaks at the active site of the enzyme. In the oxidized crystals, a difference map revealed density that can accommodate a linear molecule comprising at most three atoms adjacent to the type 2 copper sites in subunits A and B. Nitrous oxide molecules were refined bound side-on to these coppers (Figure 1E). The X-ray data were insufficient to distinguish between the oxygen and the nitrogen atoms.

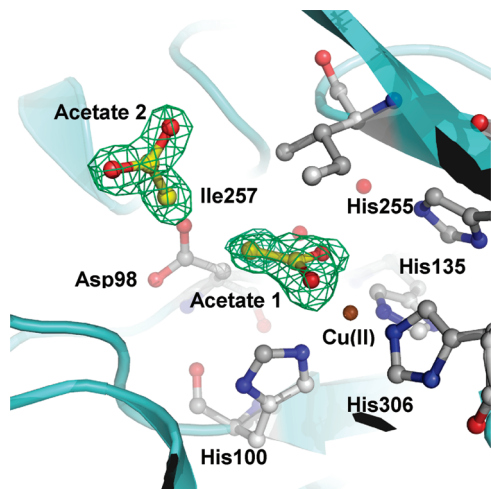


FIGURE 2: Acetate molecules bound in close proximity to the type 2 copper site of *AfNiR*. Acetate 1 interacts with the copper and acetate 2 is located within 4 Å from acetate 1. Carbon atoms of the bound inhibitors are colored in yellow, and the carbon atoms of the protein are colored in gray. The omit difference electron density map for both acetate molecules is represented in green and contoured at  $4.5\sigma$ .

By contrast, the density in subunit C was modeled as an acetate molecule bound at the active site. The presence of acetate in these crystals is likely due to the presence of 100 mM acetate at pH 4 in the crystallization buffer. The three active sites of *AfNiR* differ in accessibility due to crystal packing which likely results in the observed variation in binding at each type 2 site. In subunits A and B, the side chain of Asp98 is displaced to point away from the copper ion to accommodate the bound nitrous oxide. The average *B*-factor of the nitrous oxide molecules at full occupancy in subunits A and B is 31 Å<sup>2</sup>.

Up to eight additional bound anions were observed in all structures of *AfNiR*. The bound anions were modeled as acetate molecules, consistent with the inclusion of 0.1 M acetate in the crystallization buffer. However, the identity of each of these bound anions was not independently verified in all enzyme–inhibitor complexes. One of these additional anion binding sites is located in the deep active site cavity approximately 7 Å from the type 2 copper. In the structures of *AfNiR*–inhibitor complexes, this site occurs 4 Å from the bound inhibitor (Figure 2) but was not consistently occupied in each subunit. With the exception of the *AfNiR*–nitrate complex, the acetate molecule was located and oriented the same way and is stabilized by hydrophobic interactions with the protein and a hydrogen bond to a nearby, enzyme-bound water molecule. In the structure of the *AfNiR*–nitrate complex, the acetate molecule is located 1 Å further away from the active site, likely due to steric clash with the bound nitrate. No other bound anions were observed in the active site cleft in any of the enzyme–inhibitor complexes.

**Steady-State Turnover of *AfNiR*.** The turnover of *AfNiR* was analyzed at each of pH 4 and 6.5 under steady-state conditions by monitoring the oxidation of reduced pseudoazurin (see Supporting Information, Figure S2). At both pH 4 and 6.5, the oxidation of pseudoazurin obeyed Michaelis–Menten kinetics. Although the turnover of *AfNiR* was approximately 60-fold higher at the higher pH, the enzyme's

$K_m$  for nitrite was approximately 20-fold higher, such that the difference in  $k_{cat}/K_m$  at the two pHs was only 3-fold (Table 3).

**Inhibition Parameters.** At pH 6.5, azide, formate, nitrate and acetate each inhibited the *AfNiR*-catalyzed oxidation of pseudoazurin. This inhibition was studied as a function of inhibitor and nitrite concentrations. The enzyme's  $K_m$  for nitrite and  $k_{cat}$  were relatively independent of the inhibitor, indicating the consistency of these experiments. Overall, azide inhibited *AfNiR* approximately 2 orders of magnitude more strongly than any of other three small anions (Table 3). Moreover, based on the quality of the fits using the program LEONORA (22), azide was the only investigated anion that competitively inhibited *AfNiR* with respect to nitrite. The competitive inhibition mode is also consistent with the parallel lines obtained in the Cornish–Bowden plot (Figure 3A). Similar analyses revealed that of the other three inhibitors, formate and acetate inhibited *AfNiR* in a mixed fashion and nitrate inhibited the enzyme uncompetitively (Figure 3B, C and D). Nevertheless, even the inhibition parameter for azide, the best inhibitor, was about an order of magnitude greater than the enzyme's  $K_m$  for nitrite at pH 6.5.

## DISCUSSION

The structural and kinetic studies herein demonstrate that a number of small molecules interact with the oxidized type 2 copper site of *AfNiR* and inhibit the enzyme. More specifically, the structural data show that formate, acetate, nitrate, azide and nitrous oxide bind to the catalytic center of *AfNiR*. Consistent with the structural data, those small molecules that were tested inhibited the pseudoazurin-dependent reduction of nitrite by *AfNiR*. However, the kinetic data indicate that none of the inhibitors interact as strongly with the enzyme as either nitrite or nitric oxide: the inhibition parameters were 1 to 2 orders of magnitude greater than the  $K_m$  of the enzyme for nitrite as well as the  $K_d$  of a homologue, *AxNiR*, for nitrite (31). Of the small molecules studied herein, only the inhibition of NiR by azide has been reported previously. The relatively high  $K_i$  values reported here are consistent with those studies. Thus, 1 mM azide did not detectably inhibit *AfNiR* at pH 6.3 (19) and 100 mM azide inhibited *AcNiR* at pH 6.2 by approximately 33% (32). Finally, 0.5 M azide altered the EPR spectrum of oxidized *AxNiR* at pH 8, suggesting that it binds to the type 2 copper under these conditions (33).

The current structural and kinetic data corroborate and expand previous data indicating that NiR binds small anions more strongly at lower pH. Thus, the observation that the  $K_m$  of *AfNiR* for nitrite is over an order of magnitude lower at pH 4 than at 6.5 (Table 3) is consistent with the pH-dependence of the  $K_m$  reported for *AfNiR* and *AxNiR* (7, 31). Similarly, the  $K_d$  of *AxNiR* for nitrite is at least an order of magnitude lower at pH 5.2 than at pH 7.5 (31). Finally, these data are consistent with the full occupancy of the small anionic inhibitors at the type 2 copper at pH 4 despite the use of inhibitor concentrations (20 mM) in these experiments that were up to an order of magnitude lower than the  $K_i$ 's determined at pH 6.5. The pH-dependence of the affinity of the type 2 Cu for anions could be due to changes in the reduction potential of the metal, alterations of the copper

Table 3: Steady-State Kinetic Parameters of *Af*NiR for Nitrite and Various Inhibitors<sup>a</sup>

	$k_{\text{cat}}$ ( $\text{s}^{-1}$ )	$K_{\text{m}}$ ( $\mu\text{M}$ )	$k_{\text{cat}}/K_{\text{m}}$ ( $10^6 \text{ M}^{-1} \text{ s}^{-1}$ )	$K_{\text{ic}}$ (mM)	$K_{\text{iu}}$ (mM)
pH 6.5	620 (10)	150 (10)	4.1 (0.2)		
pH 4.0	10.5 (0.3)	8 (1)	1.3 (0.2)		
azide	540 (20)	100 (10)	5.4 (0.3)	2.0 (0.1)	
formate	610 (10)	140 (10)	4.4 (0.1)	150 (10)	53 (2)
nitrate	430 (20)	110 (10)	3.9 (0.2)		61 (5)
acetate	770 (30)	230 (20)	3.3 (0.1)	160 (20)	72 (6)

<sup>a</sup> Experiments in the first two rows contained no inhibitors and were performed at the indicated pH. Inhibition experiments were performed using 50 mM MES buffer, pH 6.5. All  $K_{\text{m}}$  and  $k_{\text{cat}}/K_{\text{m}}$  values are for nitrite. Errors are indicated in parentheses.

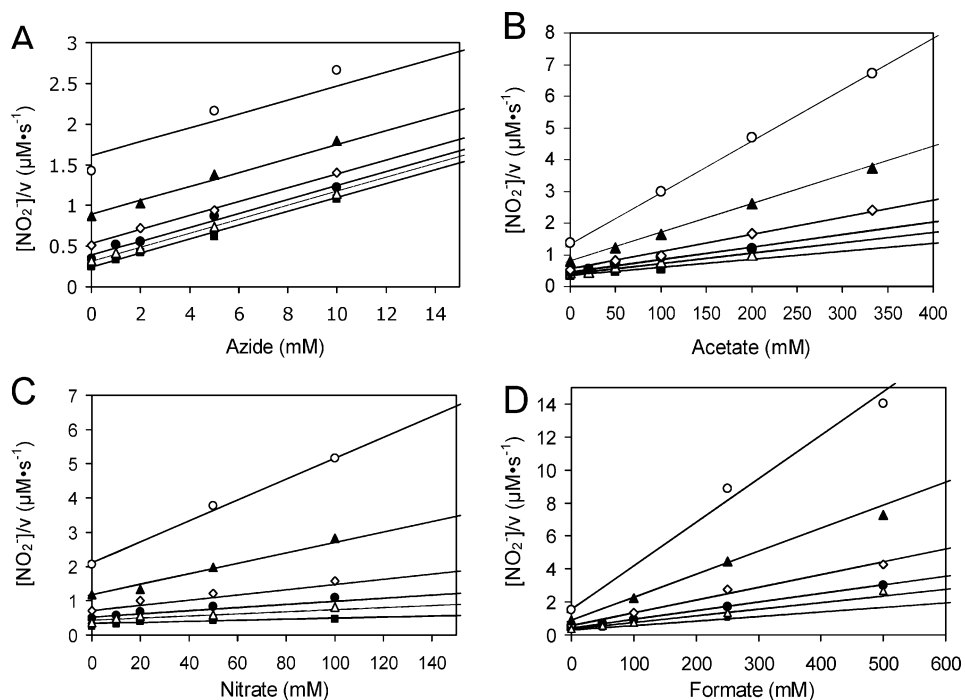


FIGURE 3: Cornish–Bowden plots of the inhibition of the *Af*NiR-catalyzed reduction of nitrite by azide (A), acetate (B), nitrate (C) and formate (D). The reaction mixtures at 25 °C contained 230 pM *Af*NiR, 315  $\mu\text{M}$  reduced pseudoazurin together with the following concentrations of nitrite: ■, 40  $\mu\text{M}$ ; △, 80  $\mu\text{M}$ ; ●, 120  $\mu\text{M}$ ; ◇, 200  $\mu\text{M}$ ; ▲, 400  $\mu\text{M}$ ; ○, 800  $\mu\text{M}$ . The indicated lines were calculated at each nitrite concentration using the parameters evaluated for entire data set as described in Experimental Procedures.

site geometry to more distorted tetrahedral geometry at higher pH (34), or, as discussed below, the protonation state of Asp98 (35). The structural data at pH 4.0 provide a rationale for the kinetic data at pH 6.5 inasmuch as the poorer inhibitors bind at a greater distance from the copper ion and have fewer specific interactions with active site residues.

The structural studies establish that formate, acetate and nitrate each bind to the type 2 copper of *Af*NiR in a bidentate, asymmetric manner as observed for nitrite (8). More specifically, in the crystal structures of these *Af*NiR–inhibitor complexes, two oxygen atoms of the bound anion are directed toward the type 2 copper in a bidentate-like manner and the water molecule that occupies the fourth coordinating position in the resting state enzyme (3) is displaced. Moreover, one of the Cu–O distances is longer than the other. The similar mode of binding of these three inhibitors and the substrate is not surprising considering the similar structures and charges of the four anions. The observed asymmetry is apparently determined by the protein environment as symmetric, bidentate binding is observed in model complexes. For example, in biomimetic compounds of carbonic anhydrase acetate bound in a bidentate symmetric manner in which the Cu–O bond distances were 2.0 Å (36). In another series of compounds, nitrate and acetate bound

the copper ion in a monodentate fashion (37). Overall, these results suggest that, in addition to determining the substrate specificity of the enzyme, the protein environment of *Af*NiR determines the mode of binding of these small inhibitors.

In light of the underlying similarities of inhibitor and nitrite binding in *Af*NiR, it is striking that the enzyme has such a low affinity for the former. More specifically, the inhibition constants for formate, acetate and nitrate were >50 mM (Table 3). By contrast, both the  $K_{\text{m}}$  and the  $K_{\text{d}}$  of NiR for nitrite (31) are 2 orders of magnitude lower. The relatively low affinity of *Af*NiR for nitrate is consistent with pulse radiolysis and EPR spectra of *Ac*NiR and *Ax*NiR. Exposing *Ac*NiR and *Ax*NiR to 16 mM solutions of nitrate altered the type 2 copper EPR spectrum and reduction potential (38). Comparison of the structures of the *Af*NiR–inhibitor complexes with that of the *Af*NiR–nitrite complex reveals two elements of the active site that apparently tune the enzymes specificity for nitrite (Figure 4A). First, the Cu–O<sub>c</sub> distances in the inhibitor complexes are ~0.15 Å longer than in the nitrite complex (Table 2). Second, Asp98 is orientated differently in the inhibitor and substrate complexes, respectively. These differences are most clear in the nitrate and acetate complexes, in which the side chain of Asp98 is orientated away from the bound inhibitor such that a

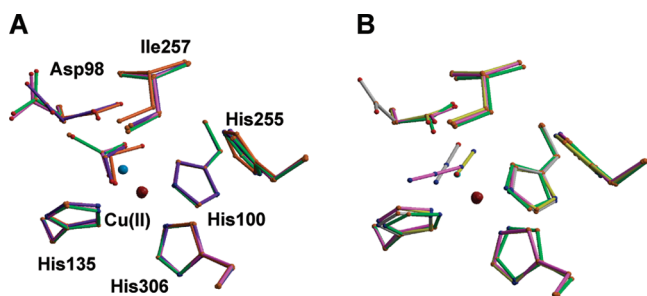


FIGURE 4: Superposition of inhibitor-bound AfNiR structures. (A) Inhibitors with two oxygen atoms for bidentate coordination. The carbon atoms of the formate-bound structure are colored in purple, of the nitrite structure are colored in orange, of the acetate structure are in pink and of the nitrate structure are in green. The oxygen and nitrogen atoms are represented as red and blue spheres, respectively. (B) Azide and nitrous oxide. The carbon atoms of the nitrous oxide structure are colored in gray, the NO structure are in yellow, the azide structure are in pink and the resting state of the enzyme is colored in green. The water molecule coordinating to Cu(II) in the resting state of the enzyme is colored in cyan.

hydrogen bond formation is not feasible. This alternate orientation is likely due at least in part to the fourth non-hydrogen atom that is present in nitrate and acetate versus nitrite and formate. Examination of the AfNiR–nitrite complex indicates that a fourth atom cannot be accommodated in the active site without displacement of the Asp98 side chain. Nevertheless, even in the AfNiR–formate complex, Asp98 clearly occupies two conformations suggesting that this residue does not interact with the inhibitor as it does with the substrate.

A second anion was bound in the cleft leading to the type 2 copper site in all but one of the NiR-complex structures. Even though an acetate molecule was modeled in that position, similarly shaped anions could likely occupy this site, providing a potential rationale for the uncompetitive component of inhibition observed for acetate, formate and nitrate. Thus, occupancy of this site by these anions would perturb diffusion of nitrite to the active site, and NO away from it. Indeed, the kinetic data suggest that at pH 6.5 all three of these inhibitors bind more tightly at this second site than at the type 2 copper. The lack of an uncompetitive component of inhibition by azide may reflect either the linear nature of this anion which may preclude its binding at the second site or the relatively lower anion concentrations used in these experiments.

The current study is consistent with previous work establishing the key catalytic role of Asp98 in AfNiR (10). In the proposed mechanism for NiR, Asp98 is deprotonated in the resting state enzyme, thereby favoring the binding of protonated substrates (10, 35). Even though its  $pK_a$  is 3.4, nitrite binds in its protonated form (15), and forms a hydrogen bond with O $\delta$ 1 of Asp98. The proposed protonation state of Asp98 is supported by FTIR spectroscopic studies of carbon monoxide binding to reduced forms of wild-type and D98N variant of AfNiR (35). In the reduced product-bound AfNiR complex, electron transfer from the copper ion to NO likely results in the generation of HNO. The proton acquired by the NO $^-$  would facilitate hydrogen bonding with the deprotonated Asp98 (9). The importance of this hydrogen bond for the formation of a stable copper–nitrosyl is further supported by density functional theory (DFT) calculations (39). The protonation states of the

formate, nitrate and acetate molecules bound to AfNiR are unknown. However, the orientation of the Asp98 side chain in the inhibitor complexes indicates that these small molecules do not form a hydrogen bond with the residue. In particular, the disorder of the side chain in the formate-bound AfNiR structure is strikingly similar to that observed in the oxidized D98N variant complexed to nitrite (10).

Significantly, the monodentate N-coordination of azide is unique among the tested inhibitors of AfNiR and is very similar to that observed in the type 2 copper site of Cu, Zn superoxide dismutase (SOD). In the reduced state, the SOD copper ion is coordinated by three histidyl residues in an approximately tetrahedral arrangement (40) as is the type 2 copper of NiR. A fourth histidine of SOD that bridges the copper and zinc sites superimposes with His255 of NiR (3, 33). Consistent with the similar structure of the copper sites of these enzymes, AxNiR has SOD activity (33). An X-ray crystallographic study revealed that azide binds bent as a fourth ligand to the Cu(II) form of yeast SOD in a manner thought to mimic superoxide (40). In the structure of the SOD–azide complex, the Cu–N $_c$  distance was 2.15 Å. EXAFS studies of a bovine SOD–azide complex revealed a shorter Cu–N $_c$  distance of 1.99 Å, in very close agreement with that reported by EXAFS studies on the AxNiR–azide complex (33) and that observed in the AfNiR–azide complex. However, the Cu–N–N angle is much more acute in SOD (<135°) (41) than in AfNiR (168°) (Figure 1A).

The binding of nitrous oxide to AfNiR clearly resembles the side-on binding of nitric oxide, and not the end-on binding of azide, despite the fact that the latter and nitrous oxide are linear and triatomic. The binding of nitrous oxide to NiR is consistent with the observation that AcNiR can catalyze the further reduction of nitric oxide to nitrous oxide in the presence of a chemical reductant (42). It is not possible to distinguish between the distal N and O atoms of the nitrous oxide molecule in the crystal structure. Nevertheless, the side-on binding of the nitrous oxide molecule is very similar to nitric oxide (Figure 4B) except that the former binds at a slightly further distance from the metal than the latter (~0.15 Å, Table 2) and interacts with the oxidized rather than the reduced form of the metal. Finally, the disorder in the side chain of Asp98 observed in this structure further suggests the critical role of this residue in discriminating between substrates and other metabolites by AfNiR.

In conclusion, the studies with small molecule inhibitors illustrate the importance of the protein environment for tuning the specificity of the copper site of NiR for reacting with nitrite. Specifically, Asp98 and Ile257 form a pocket that limits the binding of exogenous ligands. Asp98 imposes a requirement for a hydrogen bond partner, and Ile257 places steric constraints on bound ligands. Inhibitor studies with mutant forms of Asp98 and Ile257 would further confirm the importance of these residues in discriminating against binding of noncatalytic small molecules to the type 2 copper of NiR.

## SUPPORTING INFORMATION AVAILABLE

Figure showing alternative binding of formate to subunits B and C of AfNiR. Steady-state Michaelis–Menten kinetics of AfNiR at pH 4 and 6.5. This material is available free of charge via the Internet at <http://pubs.acs.org>.

## REFERENCES

- Zumft, W. G. (1997) Cell biology and the molecular basis of denitrification. *Microbiol. Mol. Biol. Rev.* 61, 533–616.
- Godden, J. W., Turley, S., Teller, D. C., Adman, E. T., Liu, M. Y., Payne, W. J., and LeGall, J. (1991) The 2.3 Ångstrom X-ray structure of nitrite reductase from *Achromobacter cycloclastes*. *Science* 253, 438–442.
- Murphy, M. E. P., Turley, S., Kukimoto, M., Nishiyama, M., Horinouchi, S., Sasaki, H., Tanokura, M., and Adman, E. T. (1995) Structure of *Alcaligenes faecalis* nitrite reductase and a copper site mutant, M150E, that contains zinc. *Biochemistry* 34, 12107–12117.
- Kukimoto, M., Nishiyama, M., Ohnuki, T., Turley, S., Adman, E. T., Horinouchi, S., and Beppu, T. (1994) Identification of interaction site of pseudoazurin with its redox partner, copper-containing nitrite reductase from *Alcaligenes faecalis* S-6. *Biochemistry* 33, 5246–5252.
- Suzuki, S., Kataoka, K., Yamaguchi, K., Inoue, T., and Kai, Y. (1999) Structure-function relationships of copper-containing nitrite reductases. *Coord. Chem. Rev.* 190–192, 245–265.
- Dodd, F. E., Van Beuemen, J., Eady, R. R., and Hasnain, S. S. (1998) X-ray structure of a blue-copper nitrite reductase in two crystal forms. The nature of the copper sites, mode of substrate binding and recognition by redox partner. *J. Mol. Biol.* 282, 369–382.
- Wijma, H. J., Jeuken, L. J., Verbeet, M. P., Armstrong, F. A., and Canters, G. W. (2006) A random-sequential mechanism for nitrite binding and active site reduction in copper-containing nitrite reductase. *J. Biol. Chem.* 281, 16340–16346.
- Murphy, M. E., Turley, S., and Adman, E. T. (1997) Structure of nitrite bound to copper-containing nitrite reductase from *Alcaligenes faecalis*. Mechanistic implications. *J. Biol. Chem.* 272, 28455–28460.
- Tocheva, E., Rosell, F., Mauk, G., and Murphy, M. (2004) Side-on copper-nitrosyl coordination by nitrite reductase. *Science* 304, 876–870.
- Boulanger, M. J., and Murphy, M. E. P. (2001) Alternate substrate binding modes to two mutant (D98N and H255N) forms of nitrite reductase from *Alcaligenes faecalis* S-6: structural model of a transient catalytic intermediate. *Biochemistry* 40, 9132–9141.
- Boulanger, M. J., and Murphy, M. E. P. (2003) Directing the mode of nitrite binding to a copper-containing nitrite reductase from *Alcaligenes faecalis* S-6: Characterization of an active site isoleucine. *Protein Sci.* 12, 248–256.
- Veselov, A., Olesen, K., Sienkiewicz, A., Shapleigh, J. P., and Scholes, C. P. (1998) Electronic structural information from Q-band ENDOR on the type 1 and type 2 copper liganding environment in wild-type and mutant forms of copper-containing nitrite reductase. *Biochemistry* 37, 6095–6105.
- Olesen, K., Veselov, A., Zhao, Y., Wang, Y., Danner, B., Scholes, C. P., and Shapleigh, J. P. (1998) Spectroscopic, kinetic, and electrochemical characterization of heterologously expressed wild-type and mutant forms of copper-containing nitrite reductase from *Rhodobacter sphaeroides* 2.4.3. *Biochemistry* 37, 6086–6094.
- Kataoka, K., Furusawa, H., Takagi, K., Yamaguchi, K., and Suzuki, S. (2000) Functional analysis of conserved aspartate and histidine residues located around the type 2 copper site of copper-containing nitrite reductase. *J. Biochem.* 127, 345–350.
- Boulanger, M. J., Kukimoto, M., Nishiyama, M., Horinouchi, S., and Murphy, M. E. P. (2000) Catalytic roles for two water bridged residues (Asp98 and His255) in the active site of copper-containing nitrite reductase. *J. Biol. Chem.* 275, 23957–23964.
- Tocheva, E. I., Rosell, F., Mauk, A. G., and Murphy, M. E. P. (2007) Stable copper-nitrosyl formation by nitrite reductase in either oxidation state. *Biochemistry* 46, 12366–12374.
- Zhao, Y., Lukoyanov, D. A., Toropov, Y. V., Wu, K., Shapleigh, J. P., and Scholes, C. P. (2002) Catalytic function and local proton structure at the type 2 copper of nitrite reductase: the correlation of enzymatic pH dependence, conserved residues, and proton hyperfine structure. *Biochemistry* 41, 7464–7474.
- Wijma, H. J., Boulanger, M. J., Molon, A., Fittipaldi, M., Huber, M., Murphy, M. E. P., Verbeet, M. P., and Canters, G. W. (2003) Reconstitution of the type-1 active site of the H145G/A variants of nitrite reductase by ligand insertion. *Biochemistry* 42, 4075–4083.
- Kakutani, T., Watanabe, H., Arima, K., and Beppu, T. (1981) Purification and properties of copper-containing nitrite reductase from a denitrifying bacterium *Alcaligenes faecalis* strain S-6. *J. Biochem.* 89, 453–461.
- Brenner, A. J., and Harris, E. D. (1995) A quantitative test for copper using bicinchoninic acid. *Anal. Biochem.* 226, 80–84.
- Wijma, H., Canters, G., de Vries, S., and Verbeet, M. (2004) Bidirectional catalysis by copper-containing nitrite reductase. *Biochemistry* 43, 10467–74.
- Cornish-Bowden, A. (1995) *Analysis of enzyme kinetic data*, Oxford University Press, New York, NY.
- (1968) *Merck Index*, p 744, Merck and Co., Inc., Rahway, NJ.
- Otwinowski, Z., and Minor, W. (1997) Processing of x-ray diffraction data collected in oscillation mode. *Methods Enzymol.* 276, 307–326.
- Kukimoto, M., Nishiyama, M., Murphy, M. E. P., Turley, S., Adman, E. T., Horinouchi, S., and Beppu, T. (1994) X-ray structure and site-directed mutagenesis of a nitrite reductase from *Alcaligenes faecalis* S-6: roles of two copper atoms in nitrite reduction. *Biochemistry* 33, 5246–5252.
- Murshudov, G. N., Vagin, A. A., and Dodson, E. J. (1997) Refinement of macromolecular structures by the maximum-likelihood method. *Acta Crystallogr.* 53, 240–255.
- Lamzin, V. S., and Wilson, K. S. (1993) Automated refinement of protein models. *Acta Crystallogr. D* 49, 129–147.
- Collaborative Computational Project, N. (1994) The CCP4 suite, programs for protein crystallography. *Acta Crystallogr. D* 50, 760–763.
- Jones, T. A., Zou, J. Y., Cowan, S. W., and Kjeldgaard, M. (1991) Improved methods for building protein models in electron density maps and the location of errors in these models. *Acta Crystallogr.* A47, 110–119.
- Laskowski, R. A., MacArthur, M. W., Moss, D. S., and Thornton, J. M. (1993) PROCHECK: a program to check the stereochemical quality of protein structures. *J. Appl. Crystallogr.* 26, 283–291.
- Abraham, Z. H., Smith, B. E., Howes, B. D., Lowe, D. J., and Eady, R. R. (1997) pH-dependence for binding a single nitrite ion to each type-2 copper centre in the copper-containing nitrite reductase of *Alcaligenes xylosoxidans*. *Biochem. J.* 324, 511–516.
- Hulse, C. L., and Averill, B. A. (1989) Evidence for a copper-nitrosyl intermediate in denitrification by the copper-containing nitrite reductase of *Achromobacter cycloclastes*. *J. Am. Chem. Soc.* 111, 2322–2323.
- Strange, R. W., Murphy, L. M., Dodd, F. E., Abraham, Z. H., Eady, R. R., Smith, B. E., and Hasnain, S. S. (1999) Structural and kinetic evidence for an ordered mechanism of copper nitrite reductase. *J. Mol. Biol.* 287, 1001–1009.
- Jacobson, F., Pistorius, A., Farkas, D., De Grip, W., Hansson, O., Sjölin, L., and Neutze, R. (2007) pH dependence of copper geometry, reduction potential, and nitrite affinity in nitrite reductase. *J. Biol. Chem.* 282, 6347–6355.
- Zhang, H., Boulanger, M. J., Mauk, A. G., and Murphy, M. E. P. (2000) Carbon monoxide binding to copper-containing nitrite reductase from *Alcaligenes faecalis*. *J. Phys. Chem. B* 104, 10738–10742.
- Han, R., and Parkin, G. (1991) Unidentate versus bidentate coordination of nitrate ligands: relevance to carbonic anhydrase activity. *J. Am. Chem. Soc.* 113, 9707–9708.
- Halfen, J. A., and Tolman, W. B. (1994) Synthetic model of the substrate adduct to the reduced active site of copper nitrite reductase. *J. Am. Chem. Soc.* 116, 5475–5476.
- Suzuki, S., Deligeer, Yamaguchi, K., Kataoka, K., Kobayashi, K., Tagawa, S., Kohzuma, T., Shidara, S., and Iwasaki, H. (1997) Spectroscopic characterization and intramolecular electron transfer process of native and type 2 Cu-depleted nitrite reductase. *J. Biol. Inorg. Chem.* 2, 265–274.
- Periyasamy, G., Sundararajan, M., Hillier, I. H., Neil, A., Burton, N. A., and McDouall, J. J. W. (2007) The binding of nitric oxide at the Cu(I) site of copper nitrite reductase and of inorganic models: DFT calculations of the energetics and EPR parameters of side-on and end-on structures. *Phys. Chem. Chem. Phys.* 9, 2498–2506.
- Hart, P. J., Balbirmie, M. M., Ogihara, N. L., Nersissian, A. M., Weiss, M. S., Valentine, J. S., and Eisenberg, D. (1999) A structure-based mechanism for copper-zinc superoxide dismutase. *Biochemistry* 38, 2167–2178.
- Blackburn, N. J., Strange, R. W., McFadden, L. M., and Hasnain, S. S. (1987) Anion binding to bovine erythrocyte superoxide dismutase studies by x-ray absorption spectroscopy. A detailed

- structural analysis of the native enzyme and the azido and cyano derivatives using a multiple-scattering approach. *J. Am. Chem. Soc.* 109, 7162–7170.
42. Jackson, M. A., Tiedje, J. M., and Averill, B. A. (1991) Evidence for an NO rebound mechanism for production of N<sub>2</sub>O from nitrite by the copper-containing nitrite reductase from *Achromobacter cycloclastes*. *FEBS Lett.* 291, 41–44.
43. Kraulis, P. (1991) MOLSCRIPT, a program to produce both detailed and schematic plots of protein structures. *J. Appl. Crystallogr.* 24, 946–950.
44. Merritt, E. A., and Bacon, D. J. (1997) Raster3D: photorealistic molecular graphics. *Methods Enzymol.* 277, 505–524.

BI7020537